

# Fast-marching eikonal solver in the tetragonal coordinates

Yalei Sun and Sergey Fomel<sup>1</sup>

**keywords:** *fast-marching, Fermat's principle, eikonal*

## ABSTRACT

Accurate and efficient traveltimes calculation is an important topic in seismic imaging. We present a fast-marching eikonal solver in the tetragonal coordinates (3-D) and trigonal coordinates (2-D), *tetragonal (trigonal) fast-marching eikonal solver* (TFMES), which can significantly reduce the first-order approximation error without greatly increasing the computational complexity. In the trigonal coordinates, there are six equally-spaced points surrounding one specific point and the number is twelve in the tetragonal coordinates, whereas the numbers of points are four and six respectively in the Cartesian coordinates. This means that the local traveltimes updating space is more densely sampled in the tetragonal (or trigonal) coordinates, which is the main reason that TFMES is more accurate than its counterpart in the Cartesian coordinates. Compared with the fast-marching eikonal solver in the polar coordinates, TFMES is more convenient since it needs only to transform the velocity model from the Cartesian to the tetragonal coordinates for one time. Potentially, TFMES can handle the complex velocity model better than the polar fast-marching solver. We also show that TFMES can be completely derived from Fermat's principle. This variational formulation implies that the fast-marching method can be extended for traveltimes computation on other nonorthogonal or unstructured grids.

## INTRODUCTION

Traveltimes map generation is a computationally expensive step in 3-D Kirchhoff depth imaging. Most approaches proposed are either based on ray tracing equation or on eikonal equation (Červený, 1987; Beydoun and Keho, 1987; Vidale, 1990; van Trier and Symes, 1991). Popovici and Sethian (1997) proposed a fast-marching finite-difference eikonal solver in the Cartesian coordinates, which is very efficient and stable. The high efficiency is based on the heap-sorting algorithm. A similar idea has been used previously by Cao and Greenhalgh (1994) in a slightly different context. The remarkable stability of the method results from a specially choosing order of

---

<sup>1</sup>**email:** yalei@sep.stanford.edu,sergey@sep.stanford.edu

finite-difference evaluation, which resembles the method used by Qin et al. (1992). Alkhalifah and Fomel (1997) implemented the fast-marching algorithm in the polar coordinates, which is more accurate than its Cartesian implementation. However, the polar implementation requires velocity to be transformed from the Cartesian to the polar coordinates for each source location, which makes it inefficient. The spatial variation of grid size in the polar coordinates also makes it more difficult to handle strong velocity variation. We present a new scheme based on the tetragonal eikonal equation. Because of the specialty of the tetragonal coordinates we have chosen, this new algorithm is more accurate than the Cartesian implementation. Meanwhile, it is free of the problems associated with the polar implementation. We first derive the tetragonal coordinates eikonal equation and explain why it is more accurate than the Cartesian fast-marching eikonal solver. Then we show how to derive the same approach from Fermat's Principle using a variational formulation, which is important for extending the fast-marching method to unstructured grids. We present 2-D and 3-D results, from simple to complex model, to support our explanation.

### TETRAGONAL EIKONAL EQUATION

In the 3-D Cartesian coordinates, the eikonal equation is expressed as

$$\left(\frac{\partial t}{\partial x}\right)^2 + \left(\frac{\partial t}{\partial y}\right)^2 + \left(\frac{\partial t}{\partial z}\right)^2 = s^2, \quad (1)$$

where  $t$  stands for travelttime and  $s$  for slowness. The 2-D counterpart is given by omitting one term from the above equation.

$$\left(\frac{\partial t}{\partial x}\right)^2 + \left(\frac{\partial t}{\partial z}\right)^2 = s^2. \quad (2)$$

The Cartesian expressions have no crossing terms because of the orthogonality. If we define a tetragonal coordinate which has a transform relation (3) with the Cartesian coordinates as shown in Figure 1

$$\begin{cases} x = \frac{\sqrt{6}}{3}u \\ y = \frac{\sqrt{3}}{6}u + \frac{\sqrt{3}}{2}v \\ z = \frac{1}{2}u + \frac{1}{2}v + w \end{cases} \quad (3)$$

and then substitute equation (3) into (1) and (2), we can get the following eikonal equation in the tetragonal (3-D) and trigonal (2-D) coordinates.

$$\begin{aligned} & \frac{3}{2} \left(\frac{\partial t}{\partial u}\right)^2 + \frac{3}{2} \left(\frac{\partial t}{\partial v}\right)^2 + \frac{3}{2} \left(\frac{\partial t}{\partial w}\right)^2 - \\ & \left(\frac{\partial t}{\partial u}\right) \left(\frac{\partial t}{\partial v}\right) - \left(\frac{\partial t}{\partial u}\right) \left(\frac{\partial t}{\partial w}\right) - \left(\frac{\partial t}{\partial v}\right) \left(\frac{\partial t}{\partial w}\right) = s^2 \end{aligned} \quad (4)$$

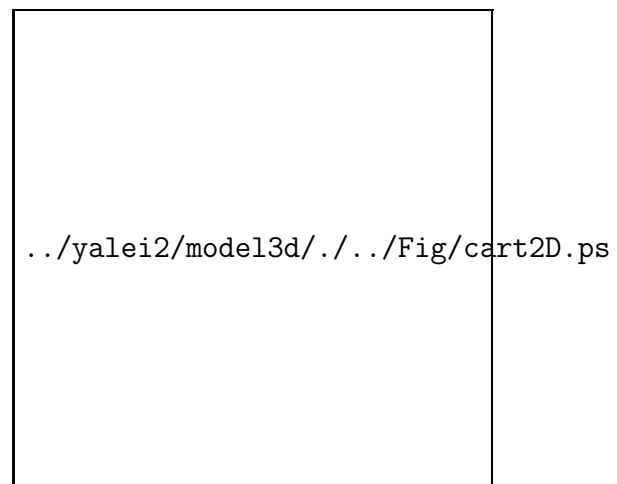
Figure 1: The tetragonal coordinates used in this paper. It reduces to the trigonal coordinates by omitting axis  $\mathbf{u}$ .



$$\frac{4}{3} \left( \frac{\partial t}{\partial v} \right)^2 + \frac{4}{3} \left( \frac{\partial t}{\partial w} \right)^2 - \frac{4}{3} \left( \frac{\partial t}{\partial v} \right) \left( \frac{\partial t}{\partial w} \right) = s^2. \quad (5)$$

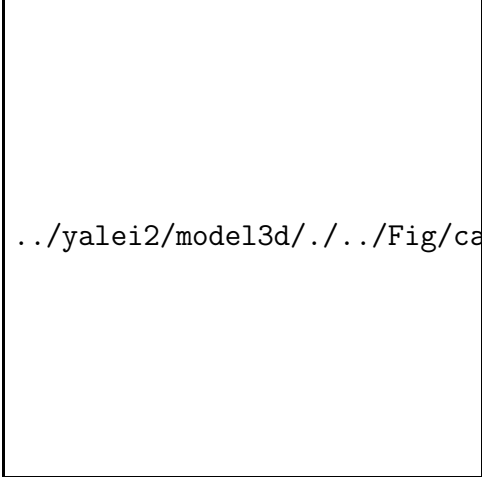
The fast-marching algorithm is an upwind first-order discretization of the above eikonal equation. In next section, we show that it reduces to solving a quadratic equation. The key feature of this algorithm is a carefully selected order of travel-time evaluation. In the Cartesian coordinates, each point with known traveltime can update four equally-spaced neighboring points in 2-D and six in 3-D, as shown in Figure 2 and 3. In the trigonal and tetragonal coordinates, these two numbers are six and twelve respectively, as shown in Figure 4 and 5. Since the fast-marching eikonal solver is based on the plane wave assumption, more equally-spaced neighboring points mean a better approximation to the assumption. Therefore, TFMES should be more accurate than its Cartesian counterpart. Alkhalifah and Fomel (1997) have shown

Figure 2: 2-D updating scheme in the Cartesian coordinates. Traveltime at point  $(i,j)$  is known and four equally-spaced neighboring points' traveltimes are candidates for updating.



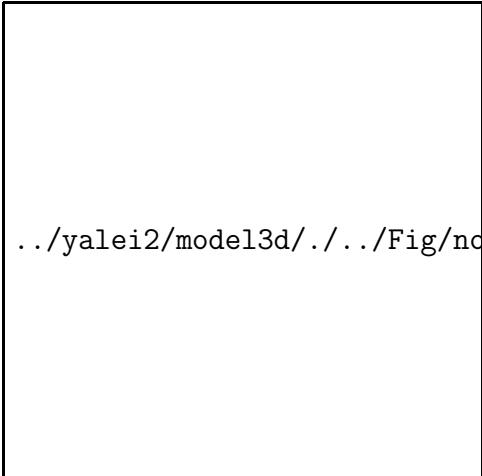
that the fast-marching algorithm in the polar coordinates is also more accurate than the Cartesian implementation. The reason is that the circular (2-D) or spherical (3-D) axis in the polar coordinates closely matches the wavefront when the media are

Figure 3: 3-D updating scheme in the Cartesian coordinates. Traveltime at point  $(i,j,k)$  is known and six equally-spaced neighboring points' traveltimes are candidates for updating.



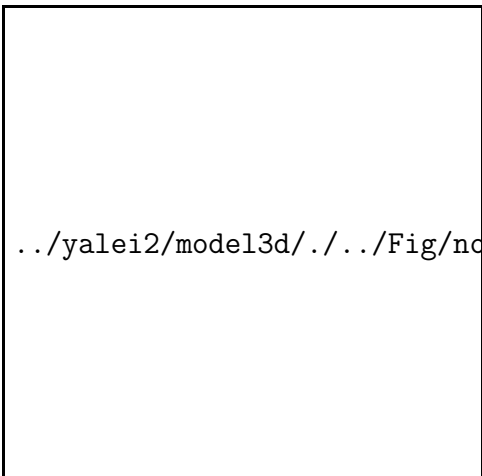
../yalei2/model3d/../../Fig/cart3D.ps

Figure 4: 2-D updating scheme in the trigonal coordinates. Traveltime at point  $(i,j)$  is known and six equally-spaced neighboring points' traveltimes are candidates for updating.



../yalei2/model3d/../../Fig/ncnorth2D.ps

Figure 5: 3-D updating scheme in the nonorthogonal coordinates. Traveltime at point  $(i,j,k)$  is known and twelve equally-spaced neighboring points' traveltimes are candidates for updating.



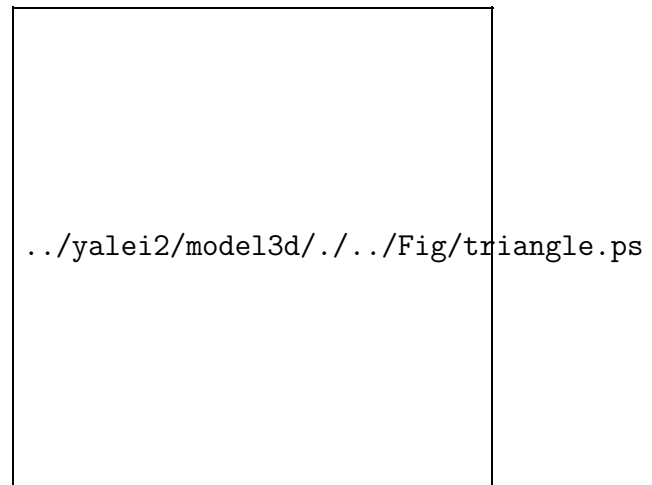
../yalei2/model3d/../../Fig/ncnorth3D.ps

relatively smooth. However, the polar implementation needs to transform the velocity model from the Cartesian to the polar coordinates for each single source, which makes it inconvenient. The grid size in the polar coordinates becomes larger and larger with the increase of radius. Therefore, some of the detailed velocity variation can be missed easily. Free of these problems, TFMES is more flexible and efficient than the polar implementation.

## VARIATIONAL FORMULATION OF FAST-MARCHING ALGORITHM

The fast-marching algorithm consists of two parts: minimum traveltimes selection and a local traveltimes updating scheme. The selection scheme is essentially based on Fermat's principle. The local traveltimes updating scheme can also be derived from the same principle using a local linear interpolation, which provides the first-order accuracy. For simplicity, let us focus on the 2-D case. Consider a line segment with

Figure 6: A geometrical scheme for the traveltimes updating procedure in two dimensions.



the end points  $A$  and  $B$ , as shown in Figure 6. Let  $t_A$  and  $t_B$  denote the traveltimes from a fixed distant source to points  $A$  and  $B$ , respectively. Define a parameter  $\xi$  such that  $\xi = 0$  at  $A$ ,  $\xi = 1$  at  $B$ , and  $\xi$  changes continuously on the line segment between  $A$  and  $B$ . Then for each point of the segment, we can approximate the traveltimes by the linear interpolation formula

$$t(\xi) = (1 - \xi)t_A + \xi t_B . \quad (6)$$

Now let us consider an arbitrary point  $C$  in the vicinity of  $AB$ . If we know that the ray from the source to  $C$  passes through some point  $\xi$  of the segment  $AB$ , then the total traveltimes at  $C$  is approximately

$$t_C = t(\xi) + s_C \sqrt{|AB|^2(\xi - \xi_0)^2 + \rho_0^2} , \quad (7)$$

where  $s_C$  is the local slowness,  $\xi_0$  corresponds to the projection of  $C$  to the line  $AB$  (normalized by the length  $|AB|$ ), and  $\rho_0$  is the length of the normal from  $C$

to  $\xi_0$ . Fermat's principle states that the actual ray to  $C$  corresponds to a local minimum of the traveltime with respect to raypath perturbations. According to our parameterization, it is sufficient to find a local extreme of  $t_C$  with respect to the parameter  $\xi$ . Equating the  $\xi$  derivative to zero, we arrive at the equation

$$t_B - t_A + \frac{s_C |AB|^2 (\xi - \xi_0)}{\sqrt{|AB|^2 (\xi - \xi_0)^2 + \rho_0^2}} = 0, \quad (8)$$

which has (as a quadratic equation) the explicit solution for  $\xi$ :

$$\xi = \xi_0 \pm \frac{\rho_0 (t_A - t_B)}{|AB| \sqrt{s_C^2 |AB|^2 - (t_A - t_B)^2}}. \quad (9)$$

Finally, substituting the value of  $\xi$  from (9) into equation (7) and selecting the appropriate branch of the square root, we obtain the formula

$$c t_C = \rho_0 \sqrt{s_C^2 c^2 - (t_A - t_B)^2} + a t_A \cos \beta + b t_B \cos \alpha, \quad (10)$$

where  $c = |AB|$ ,  $a = |BC|$ ,  $b = |AC|$ , angle  $\alpha$  corresponds to  $\widehat{BAC}$ , and angle  $\beta$  corresponds to  $\widehat{ABC}$  in the triangle  $ABC$  (Figure 6). The above general procedure can be greatly simplified when applied to some regular grids, such as the rectangular grid or the tetragonal grid. This expression is even valid for unstructured grids. As pointed out by Fomel (1997), unstructured grids have some attractive computational advantages over the regular ones. Moreover, the derivation provides a general principle, which can be applied to derive analogous algorithms for other eikonal-type (Hamilton-Jacobi) equations and their corresponding variational principles.

## NUMERICAL RESULTS

We implemented TFMES in both 2-D and 3-D cases. The 3-D constant velocity medium is used as a benchmark test to verify the accuracy of the new algorithm. We use the same sampling interval in both the Cartesian and the tetragonal coordinates to make a fair comparison. As shown in Figure 7, the Cartesian implementation tends to over-estimate the traveltime in the diagonal direction, while the tetragonal result matches the analytical result very accurately. More complex Marmousi and SEG/EAGE salt dome models are used to test its stability when handling more complex models. Figure 8 is the test of 2-D Marmousi model. The source is located on the surface at coordinates  $(x = 4100m, z = 0m)$ . In most areas, the two results match each other. When passing through the complex structure in the middle, they begin to deviate from each other. The trigonal result is not as smooth as the Cartesian result. This is because the trigonal result has six neighboring points instead of four points in the Cartesian coordinates, which makes it more capable of simulating complex wavefront. The Cartesian implementation over-estimates the traveltime compared with the trigonal result, which is similar to the conclusion reached by Alkhalifah and Fomel

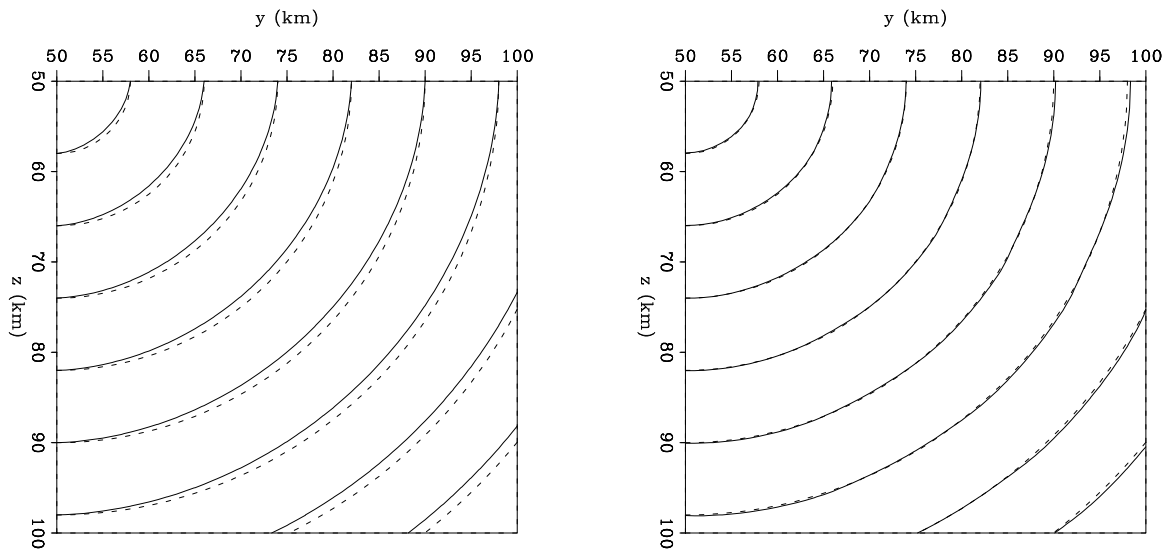


Figure 7: **Left:** Cartesian. **Right:** tetragonal. Traveltime slice from a 3-D constant velocity model. The source is located at the upper-left corner and the spatial sampling interval is 1km in all the three directions. The dash line represents the analytical solution. The solid line on the left panel stands for the Cartesian implementation and the solid line on the right for the tetragonal case. The Cartesian result has obvious errors in the diagonal direction. The tetragonal result matches the analytical result accurately. `yalei2-const3D-comp` [CR]

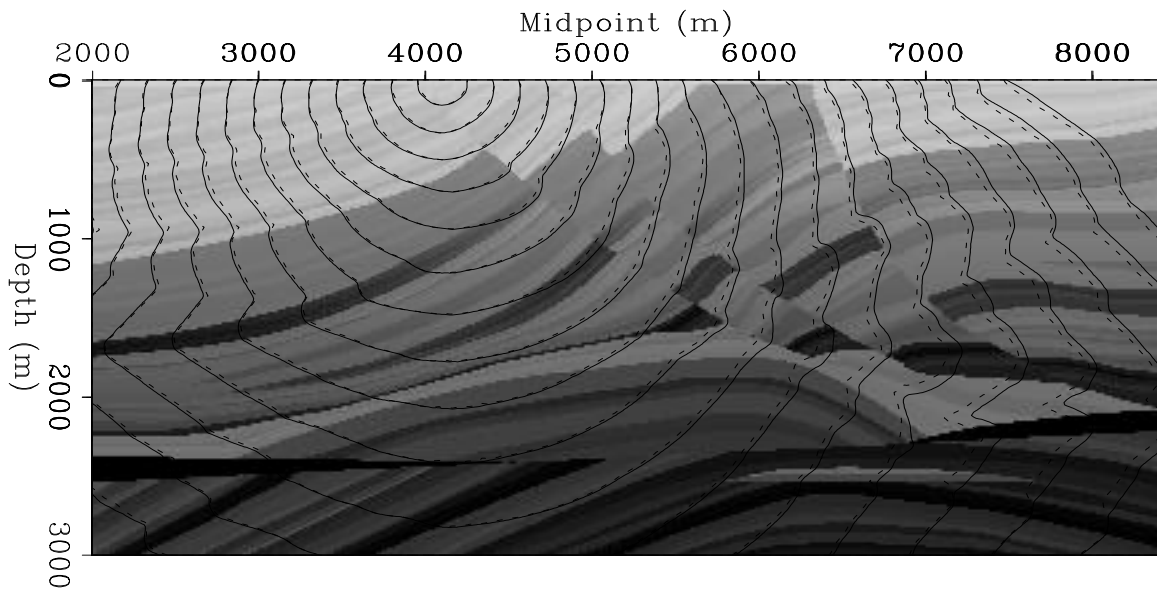


Figure 8: Traveltime slice of 2-D Marmousi model. The solid line stands for the trigonal result and the dash line for the Cartesian result. The Cartesian implementation tends to over-estimate the traveltime. `yalei2-marm-comp` [ER]

(1997). Figure 9 and 10 show three traveltime slices from the SEG/EAGE salt dome model. The source is located at coordinates  $(x = 7200m, y = 7320m, z = 1680m)$ . Figure 9 was obtained with a constant depth  $z = 1560m$ , while Figure 10 were extracted in the diagonal and anti-diagonal directions of  $x$ - $y$  plane.

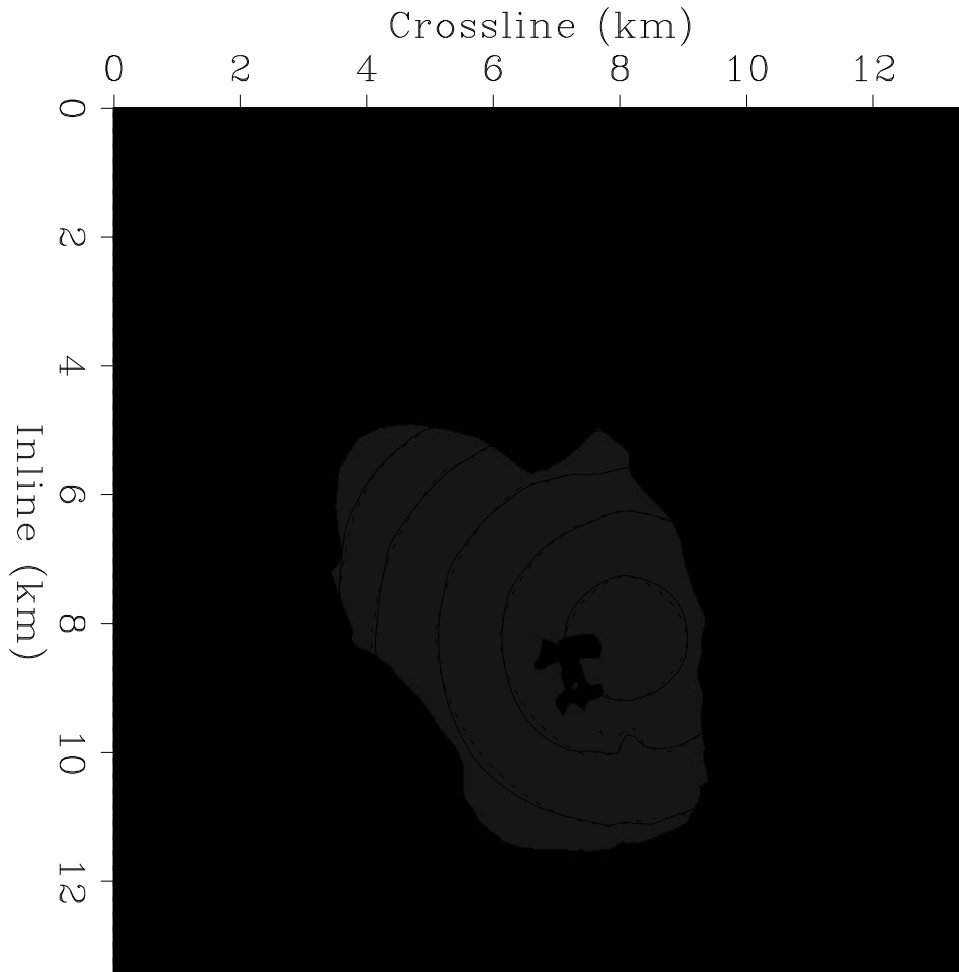


Figure 9: Traveltime slice of 3-D SEG/EAGE salt dome model for a constant  $z = 1560m$ . The solid line represents tetragonal result and the dash line for the Cartesian result. For most part, the Cartesian result tends to over-estimate the traveltime than the tetragonal result. [yalei2-salt-depth](#) [CR]

## CONCLUSION

In this paper, we extend the fast-marching eikonal solver from the Cartesian to the tetragonal coordinates. Compared with the Cartesian implementation, the tetragonal (trigonal) fast-marching eikonal solver (TFMES) can reduce the first-order approximation error. It is also more efficient than the polar implementation. Since the fast-marching eikonal solver is based on the plane wave assumption, we can derive

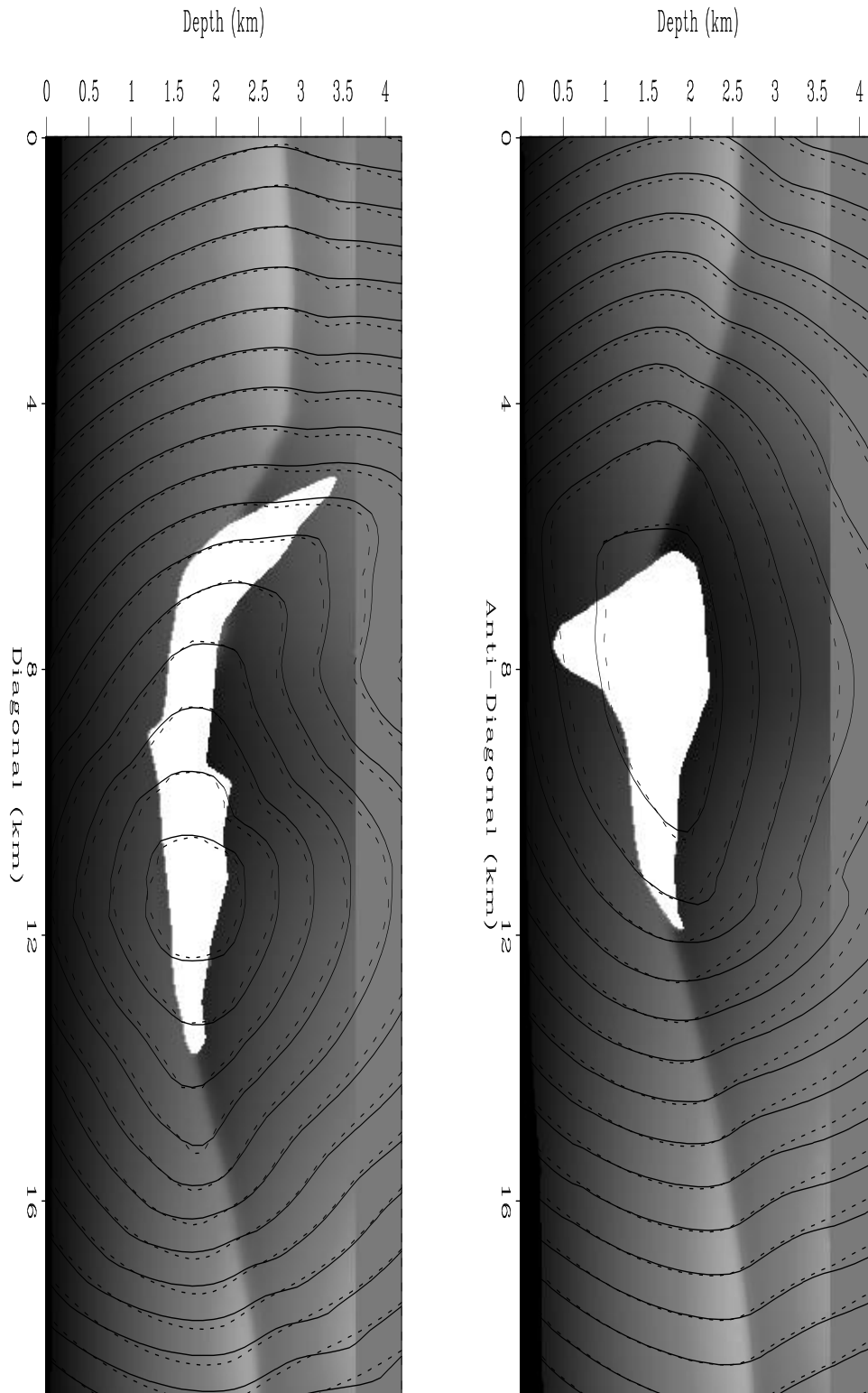


Figure 10: Traveltime slices of 3-D SEG/EAGE salt dome model in the diagonal direction. **Left:** Diagonal direction. **Right:** Anti-diagonal direction. `yalei2-salt-diag` [CR]

the same algorithm using variational principle. It is possible to extend the algorithm to unstructured grids (triangle in 2-D; tetrahedron in 3-D model).

## REFERENCES

- Alkhalifah, T., and Fomel, S., 1997, Implementing the fast marching eikonal solver: Spherical versus cartesian coordinates: SEP-**95**, 149–171.
- Beydoun, W. B., and Keho, T. H., 1987, The paraxial ray method: *Geophysics*, **52**, no. 12, 1639–1653.
- Cao, S., and Greenhalgh, S. A., 1994, Finite-difference solution of the eikonal equation using an efficient, first-arrival wavefront tracking scheme: *Geophysics*, **59**, no. 4, 632–643.
- Červený, V., 1987, Ray tracing algorithms in three-dimensional laterally varying layered structures *in* Nolet, G., Ed., *Seismic Tomography*:: Riedel Publishing Co., 99–134.
- Fomel, S., 1997, A variational formulation of the fast marching eikonal solver: SEP-**95**, 127–147.
- Popovici, A. M., and Sethian, J. A., 1997, Three dimensional traveltimes computation using the fast marching method: 67th Ann. Internat. Mtg., Soc. Expl. Geophys., Expanded Abstracts, 1778–1781.
- Qin, F., Luo, Y., Olsen, K. B., Cai, W., and Schuster, G. T., 1992, Finite-difference solution of the eikonal equation along expanding wavefronts: *Geophysics*, **57**, no. 3, 478–487.
- van Trier, J., and Symes, W. W., 1991, Upwind finite-difference calculation of traveltimes: *Geophysics*, **56**, no. 6, 812–821.
- Vidale, J. E., 1990, Finite-difference calculation of traveltimes in three dimensions: *Geophysics*, **55**, no. 5, 521–526.